Cyclic Acyclic Patterns (CAP) framework in Sleep Microstructure of Sleep Disorders: Markers of Sleep Instability Using Healthy Controls as Reference

Dimitriadis SI[1-3*], Salis CI[1,4]

[1]Integrative Neuroimaging Lab, 55133, Thessaloniki, Macedonia, Greece
[2]1st Department of Neurology, G.H. 'AHEPA', School of Medicine, Faculty of Health Sciences, Aristotle University of Thessaloniki (AUTH), 54124, Thessaloniki, Macedonia, Greece
[3]Neuroinformatics Group, Cardiff University Brain Research Imaging Centre (CUBRIC), School of Psychology, College of Biomedical and Life Sciences, Cardiff University, Maindy Rd, CF24 4HQ, Cardiff, Wales, United Kingdom
[4] Department of Electrical and Computer Engineering, University of Western Macedonia, 50131, Kozani, Macedonia, Greece

Abstract

Objective

This study aims to present a novel multi-feature Sleep Instability Score (SLEIS) for sleep disorders. We also evaluate its performance in simultaneously discriminating seven sleep disorders, employing a healthy control group as a reference.

Methods

This study extracts for the first time an exhaustive number of macrostructural and microstructural CAP sleep features from an open sleep disorder database. We assessed the deviation of sleep disorders groups from a healthy control group across all extracted features, quantifying the relevant effect size using Cohen's *d* statistic. We generated two versions of the SLEIS score, representing a) the individual feature value multiplied by the corresponding Cohen's d, and b) their cumulative weight over groups of features. We employed a Random Forest (RF) model to rank the best features that can better distinguish the seven sleep disorders, thereby identifying a novel multi-feature marker of sleep instability.

Results

RF classification on the original feature values and following an eight-class approach failed to present a robust discrimination of the sleep disorders and the healthy control group (precision = 56.44 %, recall = 60%, F1-score = 57.87%). The improvement was obvious with both versions of the SLEIS score (groups of features/individual features: precision = 95.23% / 100%, recall = 90.71% / 100%, F1-score = 92.23% / 100%).

Conclusions

Normative modeling weighting approaches for macro- and microstructural features, considering effect size as deviation from a normative sample, are of paramount importance.

Significance

Our approach provides a promising solution for determining a novel instability marker (SLEIS) that considers the heterogeneity of sleep disorders.

Keywords: cyclic alternating pattern ; sleep disorders ; microstructure ; macrostructure ; random forest ; normative modeling

***Correspondence to :**

Dr. Stavros I. Dimitriadis

Head of Integrative Neuroimaging Lab, Thessaloniki, 55133, Makedonia, Greece

Email: stidimitriadis@gmail.com

Abbreviations:

NREM - non-rapid eye movement

REM - rapid eye movement

SWS - slow wave sleep

SWA - slow wave activity

SCN - suprachiasmatic nucleus

LC - locus coeruleus

NA - noradrenaline

CAP - cyclic alternating pattern, NCAP - non-CAP , CAPs - CAP sequences

EEG - electroencephalography

LORETA - low resolution brain electromagnetic tomography

RF - Random Forest

OOB - out-of-bag (OOB) error

SLEIS - sleep instability score

Highlights (130 characters):

- We determined the deviation of sleep disorders groups from a healthy control group across multiple features, quantifying it by Cohen's *d*
- We employed normative modeling weighting approaches for CAP features, considering Cohen's *d* as deviation from a normative sample
- We demonstrated the efficacy of a novel approach to address the heterogeneity of sleep disorders by determining a novel SLEIS score

1. Introduction

The complex organization of sleep stages and their temporal evolution during the night is characterized by cyclic alterations between non-rapid eye movement (NREM) and rapid eye movement (REM) sleep stages. This statement provides a brief description of sleep architecture (Mogavero et al.,(Mogavero et al. 2025). Each of the sleep stages, including the NREM substages (N1, N2, N3, and/or N4), is distinguished by distinct physiological processes, neural activity, and electroencephalographic (EEG) patterns (Troester 2023). Neurophysiologists have perceived NREM sleep stages as periods of reduced arousal threshold, relative quiescence, and slower brain activity compared to wakefulness (Martin et al. 2020). In contrast, REM sleep is associated with heightened brain activity, rapid eye movements, and vivid dreaming (Carskadon and Dement 2005).

The temporal organization of NREM-REM cycles across the night delineates the macrostructure of sleep. A series of macrostructural parameters provides information on the timing, alterations of sleep stages, and continuity of sleep composition derived from polysomnography (see Table 1 in Parrino et al. 2021). Sleep macrostructure refers to the overall organization of sleep stages throughout the night, encompassing the duration spent in each stage (N1, N2, N3, N4 and REM) and the transitions between them. It essentially describes the "big picture" of sleep architecture, focusing on the larger patterns and durations of sleep periods. Basic macrostructure measurements are Total Sleep Time (total duration of sleep time), Sleep Latency (The time it takes to fall asleep), number of waking, NREM (N1, N2, N3, N4) - REM duration, **Sleep Efficiency** (The percentage of time in bed spent asleep), and Heart Rate (Ghermezian et al. 2023).

In mammals, the master sleep clock that regulates the harmonic alterations of sleep and wake cycles over a 24-h period is located in the suprachiasmatic nucleus (SCN) (Ma and Morrison 2025). SCN is a small region in the hypothalamus that regulates daily cycles of physiology and behavior, including the sleep-wake cycle (Moore 2007). The SCN receives light information from the eyes and synchronizes these rhythms with the external light-dark cycle, ensuring the alignment of our bodies with the 24-hour day (Mieda 2020). Many physiological functions in our body exhibit

oscillations with frequencies ranging from milliseconds to days, such as heart rate, brain electrical activity, breathing, the sleep-wakefulness cycle, and the circadian rhythm. Specifically, circadian rhythms are oscillations with an approximately 24-hour period that are evident in most physiological events in the body (Hastings et al. 2018). The SCN of the hypothalamus functions as a central circadian pacemaker in mammals that entrains to the environmental light/dark cycle, coordinating circadian rhythms across many brain areas and tissues (Mieda 2020).

As aforementioned, the SCN regulates the harmonic alterations of sleep-wake cycles over a near 24-h period and both environmental cues and genetic predisposition continuously modulate SCN's functionality (Jones et al. 2016). The contribution of environment, genes, and gene-environment interactions to sleep disorders is well established. Familial and twin sleep disorder studies revealed an important influence of genetic factors. Only four rare diseases may result from just a single mutation, and these are: familial advanced sleep-phase syndrome, fatal familial insomnia, chronic primary insomnia, and narcolepsy with cataplexy. These are called monogenic sleep disorders (Bidaki et al. 2012). However, most sleep disorders are more complex in their genetic susceptibility, including a variance in expressivity of the phenotype across the members of the same family (Dauvilliers and Tafti 2008).

FROM SLEEP MACROSTRUCTURE TO CYCLIC ALTERNATING PATTERN

Sleep macro-architecture is an ordered sequence of altered sleep stages integrated within a sleep cycle. During sleep, mammals are not totally isolated with the external world but sleep allows interactions and integrations between the external environment and the internal habitats. Arousals are not open windows of wakefulness but indicate the resistance of sleep macrostructure to potential perturbations. A single arousal doesn't have consequences on an individual's health and sleep quality. However, regarding physiological sleep, arousals often appeared as swarms and as isolated phenomena. Periodic and ordered sequences of arousals

compose the so-called cyclic alternating pattern (CAP) as they were defined by Terzano (Terzano 1991).

Terzano et al. introduced CAP on sleep research based on observations that microstructural events occur in bursts and not in isolation (Terzano et al. 1985). They divided sleep in two phases, A and B. Phase A involves phasic events that deviate from the EEG background activity and includes K-complex sequences, delta bursts, vertex sharp transients, arousals, and polyphasic bursts. Phase B represents tonic non-transient background activity. Moreover, Phase A can be subdivided into three subtypes (see Materials and Methods). Sleep in the microstructure level is classified as CAP if a phase A is followed by a B phase within 60 seconds, and as non-CAP in case only phase B is present. The most frequent statistic extracted from CAP sleep microstructure is CAP rate, which is estimated as the percentage ratio of total CAP time to total NREM sleep time (consisting of CAP + non-CAP). The heightened presence of phase A can be seen as sleep disturbances on the microstructural level, and the CAP rate can be seen as a measure of arousal instability. Higher CAP rates are associated with poorer sleep quality (Parrino et al. 2012).

Altered CAP rates have been observed in a wide range of pathological sleep conditions, including sleep apnea, insomnia, and periodic limb movements (Parrino et al. 1996, 2012; Terzano et al. 1996; Zucconi et al. 2000). Moreover, sleep-related events such as bruxism, sleepwalking, and epileptic activity seem to have a higher prevalence during phase A, while sleep apneas typically occur during phase B (Parrino et al. 2012).

The present study aims to extensively quantify CAP-related microstructural features in a healthy control group and seven sleep disorders as a way to reveal potential markers of sleep instability. We analyzed 108 polysomnographic recordings of the CAP Sleep Database contributed by the Sleep Disorders Center of the Ospedale Maggiore of Parma, Italy (Goldberger et al. 2000; Terzano et al. 2001). Our microstructural analysis focused on annotated CAP over the hypnograms

provided by Terzano's group of colleagues. We also estimated macrostructural features derived from hypnograms as a way to reveal potential complementarity with the microstructural CAP feature sets. Recent neuroimaging studies have used normative modelling approaches to detect brain disorders as deviations from normative brain age-matched charts across multiple neuroimaging modalities (Dimitriadis et al. 2019; Bethlehem et al. 2022; Dimitriadis 2022, 2024; Lancaster et al. 2022; Rutherford et al. 2022; Marquand et al. 2024; Shafiei et al. 2025). Similarly, we employ the healthy control group of this unique database as a common reference for the seven sleep disorders. In this way, we anticipate that the use of robust sleep-disorder prior effect size weights, referenced against a common healthy control group, will help parse both individual-level and disorder-specific heterogeneity by accounting for personalized profiles of macrostructural and microstructural alterations. This approach is expected to provide sleep disorder–specific sensitivity.

The remainder of this paper is organized as follows: Section 2 describes the existing CAP database and the quantified macrostructural and microstructural CAP features. Section 3 is devoted to the obtained results, and Section 4 is dedicated to the discussion of the added value and limitations of the study and the future directions of this work.

2. Materials and Methods

2.1. Material

For the purpose of our study, we downloaded all-night polysomnography (PSG) recordings from the well-known database: "The CAP Sleep Database" of "PhysioBank" (https://physionet.org/physiobank/database/capslpdb/) (Goldberger et al. 2000; Terzano et al. 2001). This study is a collection of 108 PSG recordings that include seven groups with sleep disorders and a normal healthy group that did not present any medical, neurological, or psychiatric disorder. The approval of the study

has been registered in the Sleep Disorders Center of the Ospedale Maggiore of Parma, Italy (Goldberger et al. 2000; Terzano et al. 2001). The clinical information for the whole cohort can be found in the Excel file called “gender-age.xlsx”. Sleep recordings have been annotated manually by well-trained sleep expert neurologists, based on the Rechtschaffen & Kales rules, classifying epochs as sleep stages 1–4, wake, REM sleep, and movement artifacts (Wolpert 1969). Cycling Alternating Pattern (CAP) was determined based upon Terzano’s rules (see the following section) (Terzano et al. 2001).

Table 1 summarizes the number of subjects per sleep disorder, with their gender distribution and mean age. The number of participants who were used in our study with the related sleep disorder is provided in **Table 2.**

Table 1. Demographics of the sleep disorder dataset

Sleep disorder	No. of subjects	Males	Females
Bruxism (BRUX)	2	2 (28.50 ± 7.77)	—
Sleep-disordered breathing (SBD)	3	4 (71.25 ± 7.22)	—
Insomnia (INS)	9	4 (68.00 ± 11.88)	5 (55.20 ± 4.96)
Narcolepsy (NARCO)	5	2 (33.50 ± 13.43)	3 (30.33 ± 13.05)
Nocturnal frontal lobe epilepsy (NFLE)	40	21 (27.80 ± 8.27)	19 (33.00 ± 12.87)
Periodic leg movements (PLMs)	10	7 (56.71 ± 7.54)	3 (51.33 ± 1.15)
REM behavior disorder (RBD)	22	19 (70.10 ± 6.65)	3 (74.66 ± 1.52)
No pathology (N)	16	7 (30.42 ± 3.73)	9 (33.55 ± 6.52)

Table 2. A summarization of the indices of the selected subjects per group

Bruxism	Insomnia	Healthy controls	Narcolepsy	Nocturnal frontal lobe epilepsy	Periodic leg movements	REM behavior disorder	Sleep-disordered breathing
Brux1, brux2	isn1-ins9	n1-n5, n10, n11, n16	Narco1-narco5	nfle1-nfle40	plm1-plm10	rbd1-rbd22	sdb1-sdb4

2.2 Methodological and technical requirements for scoring a CAP sequence

An important processing step before the identification of CAP is the sleep stage manual annotation from sleep experts based on conventional criteria (Wolpert 1969; Iber 2007).

2.2.1 Onset and termination of a CAP sequence

The CAP is a periodic EEG pattern activity occurring during NREM sleep stages. A CAP is characterized by cyclic sequences that are composed of a succession of CAP cycles. A CAP cycle is composed of a phase A followed by a phase B, and at least two CAP cycles are essential to form a CAP sequence. All CAP sequences begin with a phase A, which underlines cerebral activation, and end with a phase B. Phase B comprises periods of deactivation that are interspersed by two successive phase A periods with intervals shorter than one minute. The duration of each CAP phase ranges from 2 to 60 seconds. This cut-off threshold has been defined based on the observation that more than 90% of A phases that occur during NREM sleep are separated by an interval of less than 1 minute (60 seconds) (Terzano et al. 1985; Terzano 1991; Parrino et al. 2012).

CAP is the EEG translation of the reorganization of the sleeping brain that is challenged by modifications in environmental conditions. Phases A and B are the basic compounds of each CAP cycle, corresponding to levels of greater and lesser arousal, respectively (Terzano et al. 1985). When CAP appears, arousal fluctuates constantly between two distinct sleep levels. This modulation of arousal affects not only the EEG but also the autonomic, muscular, and behavioral functions, which increase during phase A and decrease during phase B (Terzano et al. 1982; Parrino et al. 2012).

CAP expresses a basic arousal modulator, which survives in conditions of severely impaired vigilance, but essentially belongs to physiological normal sleep (Steriade et al. 1994). According to current findings, CAP appears as a well-defined marker of cerebral activity occurring under conditions of reduced vigilance (sleep, coma), translating as a state of instability that involves muscle, behavioral, and autonomic functions. The absence of CAP coincides (see next sub-section) with a condition of sustained arousal stability and is defined as non-CAP.

2.2.2 Non-CAP

Below, we summarize the three rules for characterizing a period of sleep activity as a non-CAP.

1) The absence of CAP for more than a minute (> 60 seconds) is scored as a non-CAP, and it is considered a phase of stationary activity without any phasic phase A, regardless the NREM sleep stage
2) An isolated phase A that is preceded or followed by another phase A but separated by more than a minute (60 seconds) is counted as **non-CAP**.
3) The phase A that terminates a CAP sequence is classified as **non-CAP**.

2.2.3 Minimal criteria for the detection of a CAP sequence

There is no upper limit to the overall duration of the CAP sequence and to the total number of CAP cycles. In young adults, the approximate duration of a CAP sequence is 2 minutes and 30 seconds and contains, on average, 6 CAP cycles (Smerieri et al. 2007). As previously noted, a CAP sequence is defined by at least two consecutive CAP cycles (**Fig. 1**). Considering all these rules, three or more consecutive A phases must be detected in conjunction with each of the first two A phases followed by a phase B within the one minute interval (< 60 seconds) and the last A phase followed by a non-CAP interval (> 60 seconds).

[please insert Figure 1 around here]

2.2.4 General rules

Below, we summarized general rules for the definition of CAP sequence (Parrino et al. 2012).

1) A phase A is counted within a CAP sequence only if it precedes and/or follows another phase A within the time interval of 2 to 60 seconds.
2) The onset of a CAP sequence must be preceded by a continuous NREM sleep EEG period for more than 60 seconds (non-CAP), with the following three exceptions.

There is no temporal limitation:

A) before the first CAP sequence arising in non-REM sleep;

B) after a wake-to-sleep transition;

C) after a REM to non-REM sleep transition.

2.2.5 Stage shifts

Within the NREM sleep, the evolution of a CAP sequence is not interrupted by a sleep stage shift if all CAP scoring rules are satisfied. For that reason, a CAP sequence can encapsulate different phase A and B activities since CAP sequences can extend across adjacent NREM sleep stages **(Terzano 1990)**.

2.3 Types of A-Phases

A-phases can be divided in three types: (a) A1-phase is characterized by bursts of *K*-complexes or delta waves (0.5–4 Hz), (b) A2-phase has rapid (frequencies in the beta or alpha band) EEG waves that occur for 20–50 % of the total A-phase time, and (c) A3-phase is characterized by rapid waves, alpha (8–12 Hz) and beta (16–30 Hz), that occupy more than 50 % of the total A-phase time (see **Table 3**). Thus, each type of A-phase has distinct characteristics in terms of EEG frequency content and different roles and distributions within the sleep cycle. In normal sleep, each type of A-phase has a relation with the subject's age, stage, and time of sleep, while in pathological conditions, A3-phase reflects the alteration of sleep by noxious events, i.e., obstructive apnea and leg movement (Mendez et al. 2016)).

Physiologically, CAP A1 subtypes prevail in the descending branches of the first sleep cycles, and gradually decrease during the night, mirroring the decline of the homeostatic process. Conversely, CAP A2 and A3 dominate the ascending branches of sleep cycles, and can be considered as the forerunners of REM sleep (Terzano et al. 2005).

Table 3*:* EEG characteristics of the different A phases in CAP.

	% of phase A duration occupied by low-amplitude fast waves	Types of waves
A1	<20%	Delta bursts, k-complexes, vertex sharp transients, polyphasic bursts
A2	20-50%	AASM-defined arousals, polyphasic bursts
A3	>50%	K-alpha, EEG arousals, polyphasic bursts

2.4 Macrostructure and Microstructure of Sleep.

The macrostructure of sleep refers to the overall organization and timing of sleep stages over the course of the night. It focuses on the sequence and duration of different sleep stages, including NREM (non-rapid eye movement) sleep (stages N1, N2, N3) and REM (rapid eye movement) sleep, and how these stages cycle through the night. CAP coincides with a condition of physiological instability, while non-CAP translates to a condition of physiological stability. Non-CAP and CAP sequences constitute the microstructure of sleep. **Fig.2** illustrates an example from each sleep disorder with the hypnogram and the appearance of CAP sequences across the sleep stages.

[please insert Figure 2 around here]

2.5 Description of Quantitative Features Extracted based on Hypnograms and CAP

We estimated a total number of one hundred and thirteen (113) microstructural and macrostructural features. Our analysis focused on the formation of CAP sequences for the microstructural extraction of CAP-related features.

2.5.1 Macrostructural Sleep Features

This section includes the description of the eleven (11) macrostructure features.

Sleep Efficiency (%). This feature is the ratio of the total time a person spends asleep to the total duration of sleep (including also the wake state). Mathematically, Speep Efficiency can be expressed via the following equation:

$$Sleep\ Efficiency = \frac{1 - Wake}{Total\ Sleep\ Time} \quad (1)$$

where indicates the total time, the person is awake. This characteristic corresponds to 1 feature.

Ratio of Sleep Stage X to the total duration of NREM plus REM (%): This characteristic measures the percentage of time that the brain spends at the stage X to the total number of stages in NREM plus in REM. The stage X can be one of the following: stages in N1, stages in N2, stages in N3, stages in N4, total number of stages in N1 plus the stages in N2, total number of stages in N3 plus the stages in N4, stages in NREM, stages in REM. As a result, this feature yields eight (8) features. Mathematically, this ratio is calculated as follows:

$$Ratio\ of\ Sleep\ Stage\ X = \frac{X}{NREM + REM} \quad \textbf{(2)}$$

Total sleep time (minutes): This characteristic measures the total sleep time, e.g., the total sum of NREM plus the REM stages, yielding one (1) feature.

Time passed from the first N1 epoch to the first REM epoch (minutes): This feature measures the time passed from the beginning of the first N1 epoch, until the first REM epoch. As a result, this quantity yields one (1) feature.

2.5.2 Microstructural CAP features

This section describes the microstructural features. These characteristics are quantified within three distinct domains: e.g.

Domain 1 - Whole NREM sleep: Encompassing stages N1, N2, N3, and N4

Domain 2 – Light sleep: Encompassing stages N1 and N2

Domain 3 – Deep sleep: Encompassing stages N3 and N4

while in some of them, we adopted both mean and median statistical metrics. This approach leads to a total of one hundred and two (102) microstructural features. In Domains 2 and 3, our analysis focused on CAP sequences that start and end on the same sleep stage (either N1 or N2, and either N3 or N4). **Table 4** illustrates the definition of the extracted features divided in one measurement, estimation of mean/median in NREM, and also mean/median in N1/N2 and N3/N4.

CAP rate (%), defined as the ratio between the total time (in minutes) spent in all CAP sequences and the total time (in minutes) spent in NREM sleep. This feature is computed within **Domain 1** and yields one (1) feature.

CAP time (minutes), defined as the cumulative duration (in minutes) spent in all CAP sequences across NREM stages. This feature is computed within **Domain 1** and yields one (1) feature.

CAP rate in N_x (%), defined as the duration spent in all CAP sequences related to stage N_x (where N_x can be one of the following: N_1, N_2, N_3, and N_4) divided by the total duration of stage N_x. This feature is computed within **Domain 1**, resulting in four (2x2) features.

Mean/median number of CAP cycles per CAP sequence (number). This feature is computed by firstly counting the number of CAP cycles within each CAP sequence, followed by calculating both the mean and the median values of the resulting distribution. As a result, this characteristic corresponds to two (2) sub-features (mean value and median) and is extracted for each of the **Domains 1, 2, and 3**, yielding a total of six (2x3) features.

Mean/median duration of CAP cycles across sequences (seconds). This feature is computed by measuring the mean duration of all CAP cycles within each CAP sequence, followed by calculating both the mean and the median values of the resulting distribution. As a result, this characteristic corresponds to two (2) sub-features (mean value and median) and is extracted for each of the **Domains 1, 2, and 3**, yielding a total of six (2x3) features.

Mean/median duration of CAP sequences (seconds). This feature is computed by measuring the duration of each CAP sequence, followed by calculating both the mean and the median values of the resulting distribution. As a result, this characteristic corresponds to two (2) features (mean value and median) and is extracted for each of the **Domains 1, 2, and 3**, yielding a total of six (2x3) features.

Total number of CAP sequences (count). This feature is computed by measuring the number of CAP sequences across **Domains 1, 2, and 3**. As a result, three (1x3) features are generated.

Total duration of CAP sequences (minutes). This feature is computed by measuring the total duration of CAP sequences across **Domains 1, 2, and 3**. As a result, three (1x3) features are generated.

The total number of CAP cycles (count). This feature is computed by measuring the total number of CAP cycles across **Domains 1, 2, and 3**. As a result, three (1x3) features are generated.

Relative occurrence of A_x phase (%). This feature is defined as the number of A_x phases (where A_x corresponds to A_1, A_2 or A_3) divided by the total sum of $A_1 + A_2 + A_3$-- phases. As a result, this feature yields three (3) sub-features (one for each A_x phase) and is computed across **Domains 1, 2, and 3**, resulting in a total of nine (3x3) sub-features.

Mean/median duration of A_x phases (seconds). This feature is defined as the mean and the median duration of each A_x phase. The aforementioned quantity is calculated across **Domains 1, 2 and 3**, yielding two sub-features (mean and median) for each A_x phase per domain, and a total of eighteen (3x6) sub-features

Number of A_x phases per hour over NREM sleep (A index rate) in CAP sequences (number). This characteristic is computed by dividing the number of A_x phases occurring within CAP sequences by the total NREM time (in seconds) normalized to hours, e.g., NREMtime ÷ 3600. The aforementioned quantity yields three (3) sub-features (one for each Ax phase) and is computed across **Domains 1, 2, and 3**, yielding nine (3x3) features.

Number of B phases per hour over NREM sleep (B index rate) within CAP sequences (number). This characteristic is computed by dividing the total number of B phases occurring within CAP sequences by the total NREM time (in seconds) normalized to hours (NREMtime ÷ 3600). The aforementioned quantity is computed across **Domains 1, 2, and 3**, yielding three (3) features.

Mean/median duration of B phases (seconds). This feature is defined as the mean and the median duration (in seconds) of all B phases. The aforementioned quantity is computed across **Domains 1, 2, and 3**, yielding two (2) sub-features (mean and median) per domain, for a total of six (2x3) features.

Number of A_x phases per hour (number). This feature is defined as the number of A_x phases occurring within both CAP sequences and non-CAP sequences, divided by the quotient of NREM time ÷ 3600. This feature yields three (3) sub-features (one for each A_x phase) per domain and is computed across **Domains 1, 2, and 3**, resulting in a total of nine (3x3) features.

Number of B phases per hour over NREM sleep (number). This feature is defined as the number B phases occurring within both CAP sequences and non-CAP epochs, divided by the total NREM time normalized to hours (NREMtime ÷ 3600). The aforementioned quantity is computed across **Domains 1, 2, and 3**, yielding three (3) features.

Total number of A_x phases (count). This feature is defined as the total number of A_x phases occurring within both CAP sequences and non-CAP epochs. The aforementioned quantity yields three (3) sub-features (one for each A_x phase) and is computed across **Domains 1, 2, and 3**, resulting in a total of nine (3x3) features.

The total number of B phases (count). This feature is defined as the number of B phases occurring within both CAP sequences and non-CAP epochs. The aforementioned quantity is computed across **Domains 1, 2, and 3**, resulting in (3) features.

Table 4. Definition of microstructure features across three domains (NREM, light (N1/N2), and deep (N3/N4) sleep) and in both approaches using mean and median. Features with no tick means that are estimated across the sleep cycle.

	Microstructure Features							
		NREM		**N1 N2**		**N3 N4**		**Total**
Index		**Mean**	**Median**	**Mean**	**Median**	**Mean**	**Median**	
1	CAP rate (%)							1
2	CAP time (minutes)							1
3	CAP rate in Nx (%)							4
4	Mean/median number of CAP cycles per CAP sequence (number)	✓	✓	✓	✓	✓	✓	6
5	Mean/median duration of CAP cycles across sequences (seconds)	✓	✓	✓	✓	✓	✓	6
6	Mean/median duration of CAP sequences (seconds)	✓	✓	✓	✓	✓	✓	6
7	Total number of CAP sequences (count)							3
8	Total duration of CAP sequences (minutes)							3
9	Total number of							3

	CAP cycles (count)							
10	Relative occurrence of A_x phase (%)							9
11	Mean/median duration of A_x phases (seconds)	✓	✓	✓	✓	✓	✓	18
12	Number of A_x phases per hour over NREM sleep (A index rate) in CAP sequences (number)							9
13	Number of B phases per hour over NREM sleep (B index rate) within CAP sequences (number)							3
14	Mean/median duration of B phases (seconds)	✓	✓	✓	✓	✓	✓	6
15	Number of A_x phases per hour sleep (number)							9
16	Number of B phases per hour							3

	sleep (number)							
17	Total number of each A_x phase (count)							9
18	The total number of B phases (count)							3

2.6 Sleep Instability score (SLEIS) analysis

For each sleep disorder group, we considered Cohen's *d* effect size of each single feature compared to the healthy control reference group. Each participant's original feature value is then weighted by the absolute value of Cohen's *d* effect size established by the comparison of the healthy control group with the relevant sleep disorder group. The following equation (eq.3) describes the aforementioned definition in the feature level.

$$SLEIS(k,i) = \Big| feature_{value}(i) \times Cohen's\ d\ \big(control\ group(i), sleep\ disorder\ group(k,i)\big)\Big| \quad (3)$$

where (i) runs across the total number of features and (k) across the seven sleep disorder groups) and |.| indicates the corresponding absolute value.

Alternatively, we considered the aggregated Cohen's *d* effect size of the four groups of features as presented in section 2.5. The following equation (eq.4)

$$SLEIS(k, gof) = \left| \sum_{gof=1, per\ k}^{total} feature_{value}(gof) \times Cohen's\ d\ (control\ group(gof), sleep\ disorder\ group\ (k, gof)) \right| \quad (4)$$

where (k) runs across the seven sleep disorder groups, gof (group of features) runs across the ***total*** number of each distinct feature set and |.| indicates the corresponding absolute value. In both approaches, the absolute SLEIS score was taken.

This approach overcomes the low number of subjects in many sleep disorder groups, while it determines individual participant deviation from a within-sample norm tailored to the relevant sleep disorder group.

2.7 Random Forest (RF) model and experimental setup

2.7.1 RF Classifier

The RF classifier is an ensemble learning method, used extensively in classification and regression tasks (Breiman 2001). The methodology essentially involves the construction of a group (called a 'forest') of decision trees as follows: each tree in the 'forest' is built on a different training set (called a bootstrap sample), which is randomly drawn from the original training data. A randomly selected variable subset (from the original variable set) is used (during the construction of each decision tree) to establish the best split at each node. Once the RF model has been trained and all trees in the forest are constructed, their decisions are combined through majority voting (for classification) or averaging (for regression). Then, these decisions are used in predicting unknown cases.

The RF algorithm provides an internal estimator of a constructed model's generalization error, called out-of-bag (OOB) error. The estimation of the OOB error involves each decision tree in the model as follows: a portion of the original data cases (around 1/3) do not participate in the training of each tree and instead, are utilized as 'test' data, being predicted by the constructed tree. The OOB error estimate is the averaged prediction error for each training case, using only the trees that do not include that case in their bootstrap sample. For more details on the RF algorithm and its underlying notions, we refer, for example, to (Liparas et al. 2014; Dimitriadis et al. 2018a).

2.7.2 Experimental setup

In all RF models trained in our experiments, the following parameter setup was utilized: the number of trees for each model was empirically set based on the OOB error estimate. Following this approach, in all cases, the number of trees was set to 1000. For each RF model and for each node split during the growing of a tree, the number of variables used to determine the best split was set to the default $\sqrt{m}$ (m = total number of features in the dataset). In addition, the RF classifier has its own built-in feature selection method, which is to select the most important features in every RF model. Consequently, only the selected feature subsets were utilized for the training of the final RF models. Finally, a ten-fold cross-validation scheme was applied in all experiments for the training of the classifier. It is worth mentioning that the code for our RF-related experiments was written in R, version 4.3.3 (www.r-project.org/).

2.7.3 Experiments

Below, we summarize the experiments using the RF model and different combinations and definitions of our feature set.

Experiment A: We adopted the same approach as in our previous study investigating how cross-frequency coupling is altered across sleep disorders in non-CAP epochs **(Dimitriadis et al. 2021).** Specifically, we followed an eight-class classification problem (healthy control group plus seven sleep disorders) employing the whole feature set. This approach will be the reference model compared to the proposed approaches described in section 2.6 and in Experiments B and C.

Experiment B: We adopted the RF model with the four SLEIS scores corresponding to the four feature sets (eq.2) in a seven-class classification problem (seven sleep disorders). Here, we grouped the features in four sets: A) macrostructural features (11), B) CAP rates (6), C) CAP cycles and sequences (27) and D) CAP Phases A and B (69).

Experiment C: We adopted the RF model with the SLEIS scores corresponding to every single feature (eq.1) in a seven-class classification problem (seven sleep disorders).

The outcome of these experiments will quantify the importance of our approach, while it will reveal the significance of SLEIS scores in both single-feature and feature set levels.

2.8 Software

The code for the analysis of annotated hypnograms with CAP-related information has been written in MATLAB Mathworks (version 2024b). RF-related experiments have been conducted in R, version 4.3.3 (www.r-project.org/). All figures were generated in MATLAB and in the R environment.

3. Results

Prior to estimating the proposed SLEIS scores, eight features (out of 113) were excluded from the sample, because they exhibited zero values in a small number of cases. There was a small number of subjects with zero values in this set

of features, and corresponded to sleep disorder groups with a low number of samples. There was a small number of subjects with zero values in this set of features, and corresponded to sleep disorder groups with a low number of samples. As a result, the estimation of SLEIS scores was conducted with hundred and five (105) features.

3.1 Performance of the RF model with eight classes

Our RF model achieved a high performance of 87.96% on the eight-class scenario, but with a macro-average precision of 56.44%, a macro-average recall of 60 % and a macro-average *F*-score of 57.87% (**Table 5**). It is important to note that the RF model achieved the highest classification accuracy for the normal, insomnia, and NFL groups; however, no samples were classified as SDB. The OOB estimate of error rate was 51.69%. **Table 6** summarizes the confusion matrix of the RF model for the eight-class approach. The seven most discriminative features based on our RF model and with a Gini Index higher than 1 and with z-score > 1.5 across all features are demonstrated in **Fig.3**.

[please insert Figure 3 around here]

Table 5. **Precision, recall, *F*-score, and accuracy performance of the RF model for the eight-class experiment.**

Class	Precision	Recall	F-score
Ins	100 %	100 %	100 %
n	94.12 %	100 %	96.97 %
brux	NaN	0	NaN
narco	0	0	NaN
nfle	97.56 %	100 %	98.77 %
plm	88.88 %	80 %	84.21%

rbd	70.97 %	100 %	83.02 %
sbd	NaN	0 %	NaN
Macro-average	**56.44 %**	**60 %**	**57.87 %**
Accuracy	**87.96 %**		

Table 6. Confusion matrix of the RF model based on the selected features.

	Reference							
Prediction	**Ins**	**N**	**brux**	**narco**	**nfle**	**plm**	**rbd**	**sbd**
Ins	6	0	0	0	0	0	0	0
N	0	16	1	1	0	0	0	0
brux	1	0	0	0	0	1	0	0
narco	0	0	0	0	0	0	0	0
nfle	0	0	0	0	40	0	1	0
plm	1	0	0	1	0	7	1	1
rbd	1	0	1	3	0	2	20	3
sbd	0	0	0	0	0	0	0	0

3.2 Performance of the RF model with the proposed SLEIS score on the Feature Set Level

Our RF model achieved a high performance of 96.74% on the seven-class scenario, with a macro-average precision of 95.23%, a macro-average recall of 90.71 % and a macro-average *F*-score of 92.23% (**Table 7**). It is important to underline that the RF model misclassified two samples, one in rbd and one in sbd.

The OOB estimate of error rate was 9.02%. **Table 8** summarizes the confusion matrix of the RF model for the eight-class approach. Based on Gini Index and RF model, the four features sets were ranked as followed: feature set 2 (CAP rates) = 25.42, feature set 3 (CAP cycles and sequences) = 14.62, feature set 1 (macrostructural features) = 13.14, and feature set 4 (CAP Phases A and B) = 12.90. Mean and standard deviation of the four features across the sleep stages are illustrated in **Fig.4**.

[Please insert Figure 4 around here]

Table 7. Precision, recall, *F*-score, and accuracy performance of the RF model for the seven-class experiment based on the four feature sets.

Class	Precision	Recall	F-score
Ins	100 %	100 %	100 %
brux	100 %	100 %	100 %
narco	100 %	60 %	75 %
nfle	100 %	100 %	100 %
plm	100 %	100 %	100 %
rbd	91.67 %	100 %	95.65 %
sbd	75 %	75 %	75 %
Macro-average	**95.23 %**	**90.71%**	**92.23%**
Accuracy	**96.74%**		

Table 8. Confusion matrix of the RF model based on the four feature sets.

	Reference						
Prediction	Ins	brux	narco	nfle	plm	rbd	sbd
Ins	9	0	0	0	0	0	0
brux	0	2	0	0	0	0	0

narco	0	0	3	0	0	0	0
nfle	0	0	0	40	0	0	0
plm	0	0	0	0	10	0	0
rbd	0	0	1	0	0	22	1
sbd	0	0	1	0	0	0	3

3.3 Performance of the RF model with the proposed SLEIS score on the Feature Level

Our RF model achieved a high performance of 100% on the seven-class scenario, with a macro-average precision of 100%, a macro-average recall of 100%, and a macro-average *F*-score of 100% (**Table 9**). The OOB estimate of error rate was 0%. **Table 10** summarizes the confusion matrix of the RF model for the seven-class approach. The nine most discriminative features based on our RF model and with a Gini Index higher than 1 and with z-score > 1.5 across all features are demonstrated in **Fig.5**.

[please insert Figure 5 around here**]**

Table 9. **Precision, recall, *F*-score, and accuracy performance of the RF model for the seven-class experiment based on the ranked features.**

Class	Precision	Recall	F-score
Ins	100 %	100 %	100 %
brux	100 %	100 %	100 %
narco	100 %	100 %	100 %

nfle	100 %	100 %	100 %
plm	100 %	100 %	100 %
rbd	100 %	100 %	100 %
sbd	100 %	100 %	100 %
Macro-average	**100 %**	**100 %**	**100 %**
Accuracy	**100 %**		

Table 10. Confusion matrix of the RF model based on the ranked features.

```
Reference

Prediction Ins brux narco nfle plm rbd sbd

     Ins     9    0     0    0   0   0   0

     brux    0    2     0    0   0   0   0

     narco   0    0     5    0   0   0   0

     nfle    0    0     0   40   0   0   0

     plm     0    0     0    0  10   0   0

     rbd     0    0     0    0   0  22   0

     sbd     0    0     0    0   0   0   4
```

4. Discussion

In the present study, we demonstrated the efficacy of a novel method to address inter-sleep disorder variation in sleep macro- and micro-architectures by generating SLEIS scores that reflect an individual's proclivity for sleep disorder-related CAP alterations. This study extracted for the first time an exhaustive number of macrostructural and microstructural CAP sleep features from an open sleep disorder database. We determined the deviation of sleep disorders groups from a healthy control group across all estimated features, quantifying the relevant effect size using Cohen's *d* statistic. We generated two versions of the SLEIS score, representing a) the individual feature value multiplied by the corresponding Cohen's *d*, and b) their cumulative weight over groups of features. Finally, we employed a Random Forest (RF) applied over original multi-features and weighted under the two versions of the SLEIS score, as a way to evaluate its performance on the discrimination of the seven sleep disorders. The performance of our RF model with the two SLEIS scores was successful (Macro-average precision: 92.23% / 100%) ,compared to the original unweighted features (Macro-average precision: 56.44%). To our knowledge, this is the first approach to use normative modeling weighting approaches for macro- and microstructural features, considering effect size as deviation from a normative sample. Moreover, for the first time, the present study assigns cumulative weights to individual features across different sleep disorders. Therefore, we presented and assessed a novel multi-feature marker of sleep instability, the SLEIS score, demonstrating its advantages over a conventional non-weighted approach.

Sleep is a dynamic and complex process regulated by mechanisms that guide the alterations of NREM-REM sleep stages across the night. Sleep macro-architecture is characterized by the dominant slow wave sleep (SWS) (stage N3) in the first half of the night and the dominance of light sleep (N2) and REM in the second half of the night. Physiologically, this distinction of dominant sleep stages, including their distribution, is modulated by the homeostatic process and by the systems that turn on/off the REM (Brown et al. 2012). During the night, numerous

transitions occur among these sleep stages, and brain activity alters in both amplitude and frequency over seconds and minutes. The detection of the sleep stages (NREM-REM) from an EEG recording during the night is fundamental for the construction of a hypnogram. The individual hypnogram supports the identification of CAPs, which are the main electrophysiological biomarker of sleep instability (Parrino et al. 2012).

The CAP is a physiological EEG activity that is observed during NREM sleep stages and consists of repeatable spontaneous sequences of frequency/amplitude variations (phase A), which deviates from the background activity of the ongoing sleep stage and recur at intervals up to 60 seconds long. Phase A of a CAP is followed by phase B, which is characterized by a return to background activity. Both phases A and B can last between 2 and 60 seconds, and both form a CAP cycle. A succession of CAP cycles defines a CAP sequence, which is usually formed by 5-6 CAP cycles. A CAP sequence could start and end in different sleep stages (Smerieri et al. 2007).

The absence of CAP for more than 60 seconds is scored as non-CAP (NCAP), and is considered a phase of stationary activity (without any phasic CAP-A event), regardless of the NREM sleep stage (Halász et al. 2014). Based on the distribution of slow and fast EEG frequencies and the relevant phasic events of the microstructure of the sleep (delta bursts, K-complexes), A phases are classified in three subtypes: A1, A2, and A3 (Terzano et al. 2001). These phase A subtypes are not randomly distributed during the night, but instead their appearance is linked to the homeostatic, circadian, and ultradian mechanisms of sleep regulation (Parrino et al. 1993; Terzano et al. 2005; Halász et al. 2014).

Night sleep is characterized by several NREM-REM sleep cycles. Within every sleep cycle, we observe a deepening tendency from stage N1 to N4, followed by an ascending sequence of sleep stages from N3 toward stage N1 and finally the REM sleep (Halász 2016). The CAP is considered a precursor of REM sleep; it

contributes to the temporal sequence and alteration of NREM-REM sleep cycles, and for these reasons, its metrics are essential for the understanding of sleep dynamics. In the light of physiology, CAP A1 subtypes dominate the deepening branches of the first sleep cycles, and gradually decrease during the night, following the decline of the homeostatic processes. In contrast, CAP A2 and A3 prevail the ascending branches of sleep cycles and can be seen as the precursors of REM sleep (Terzano et al. 2005). CAP A1 mostly consists of slow-wave activity (SWA), which is characterized by highly synchronized cortical neurons within the delta frequency range [0.5 - 4] Hz. SWA is elaborated in the downscaling of synaptic strength, which benefits network and cellular performance (Ferri et al. 2008; Cirelli and Tononi 2022).

The aforementioned description of sleep architecture and the relevant complex patterns of fluctuated activity suggest an underlying tuning to criticality (Lo et al. 2004; Assadzadeh and Robinson 2018; Wang et al. 2019; Lombardi et al. 2020). Neuronal avalanches are defined as cascades and bursts of neural activity that exhibit power-law size and duration distributions. Therefore, neuronal avalanches can be recognized as a hallmark feature of critical dynamics in the sleep brain. A recent sleep study investigated the criticality of neuronal avalanches in normal human sleep and their relationship with sleep macro- and micro-architecture (Scarpetta et al. 2023). The authors proved that avalanche dynamics are modulated by the NREM-REM sleep cycles and that scale-free neuronal avalanche occurrence within NREM sleep stages correlates with CAP activation phases. The aforementioned work demonstrated a a potential functional link between CAP phases and brain tuning to criticality. In detail, neuronal avalanches' occurrence: a) increases in N2-N4 sleep stages during sleep deepening periods, b) decreases during the ascending branch of sleep from N4 toward stage N1, and c) correlates with the occurrence of CAP phase A, with stronger/weaker positive correlations with CAP A1 subtypes/CAP A2, A3 subtypes. SWA and the appearance of CAP-A1 phases play an important role in the sleep-dependent learning processes (Ferri et al.

2008). For that reason, a functional link between avalanche dynamics and sleep-dependent cognitive/learning processes seems logical (Scarpetta et al. 2023).

On one hand, CAP can reflect a reaction of the sleeping brain to any endogenous or exogenous disturbance. On the other hand, the CAP A phase has been interpreted as a kind of gate through which pathological events more easily occur (Parrino et al. 2006). CAP is a physiological component of NREM sleep that is observed in normal individuals (Terzano et al. 1985), demonstrating age-dependent features across the lifespan (Parrino et al. 1998). Increased amounts of CAP are often observed in sleep-disordered breathing (SDB), as well as in insomnia (Terzano et al. 2003), in sleep movement disorders (periodic leg movements (PLM) (Parrino et al. 1996), restless leg syndrome (RLS) (Hening 2004)), in bruxism ((Zucconi and Ferini-Strambi 2000; Kato et al. 2003), in parasomnias like REM behavior disorder (RBD), and in epileptic diseases such as nocturnal frontal lobe epilepsy (NFLE) (Zucconi and Ferini-Strambi 2000; Kato et al. 2003). Abnormal amounts of CAP can also be found in hypersomnias such as narcolepsy (Terzano et al. 2006; Poryazova et al. 2011).

In normal sleepers, the frequency of occurrence of arousals is higher during CAP (40/hour) compared to total sleep time (18/hour), NREM sleep (20/hour), and REM sleep (12/hour) (Terzano et al. 2002). However, CAP is not only an ‘attractor’ of arousals, but also organizes the distribution of K-complexes and delta bursts in NREM sleep. If arousals overlap with CAP phase subtypes A2 or A3, then the CAP rules allow a more concrete evaluation of sleep instability, which is characterized by delta bursts, K-complexes, and CAP phase subtypes A1. For that reason, the restriction of sleep consolidation to arousals neglects important cortical-subcortical phenomena, which are parts of a complex spatiotemporal structural pattern (Parrino et al. 2012; Scarpetta et al. 2023) .

The locus coeruleus (LC), a small nucleus in the brainstem, serves as the primary source of noradrenaline (NA) for the entire central nervous system. It is

capable of neuromodulating distinct brain regions and functions (attention, arousal, stress responses) precisely in time (Breton-Provencher et al. 2021). LC is the main component of the ascending arousal system, and functions in parallel to other cholinergic and monoaminergic nuclei to regulate sleep stages and wakefulness (Saper et al. 2010). During NREM sleep, the LC is characterized by infra-slow oscillatory activity (0.01-1 Hz) with a periodicity of around 30–50 seconds (Kjaerby et al. 2020). The time framework of LC's functionality overlaps with CAP's timescale, and this temporal alignment could suggest a functional interaction between CAP dynamics and LC-driven noradrenergic rhythms (Kjaerby et al. 2020).

In the present study, we attempted to reveal a multi-feature marker of sleep instability, focusing on the CAP sequences and on complementary macrostructural features. We aimed to define and evaluate a common sleep instability marker across seven sleep disorders, by employing the healthy control group as a common reference. For that purpose, we considered the effect size of every feature size as deviation from a normative sample, and we finally weighted individual features across various sleep disorders both individually and cumulatively in groups of features. Therefore, we presented and evaluated a novel multi-feature marker of sleep instability called the SLEIS score above a conventional non-weighted approach. Our RF model, in conjunction with both versions of SLEIS, outperformed non-weighted features and achieved an absolute performance in the individual approach (100%).

Our analysis focused on investigating microstructural and macrostructural features both qualitatively and quantitatively for the discrimination of sleep disorders from healthy controls and also between them. SLEIS score can be considered as a general sleep instability index that is simultaneously sensitive to various sleep disorders. It can be also applied as a neurophysiological marker of disorders of arousal in parasomnias sleep disorders (e.g. NFLE, RBD) complementing current knowledge over the macro- and microstructural alterations (Bergmann et al. 2024).

It is of paramount importance to investigate the dynamics relevant to CAP function, the relationship between neuronal avalanches, sleep architecture, self-organization to criticality (Scarpetta et al. 2023). Complementary, we should explore the EEG frequency components of CAP like the distribution of frequencies across the scalp and virtual sources, and their dominant frequency band in the infraslow activity (Onton et al. 2016). CAP A phases, as previously noted, exhibit distinct frequency ranges: A1 (0.25–2.5 Hz) and A3 (7–12 Hz). Source localization using low-resolution brain electromagnetic tomography (LORETA) indicates that A1 generators are mainly in the frontal midline cortex, whereas A3 generators are distributed across midline and hemispheric parietal and occipital regions. The structural coordinated association between those two different CAP frequency components located in anatomical distant brain areas is indicative of the functional intercoupling of those two frequency components. This functional intercoupling could be altered in sleep disorders.

Limitations

The first limitation of the present study is related to the number of samples per sleep disorder and the underrepresentation of certain sleep disorder classes. Secondly, our analysis focused on annotated epochs for both sleep stages (W/N1/N2/N3/N4/REM) and CAP phases (A1/A2/A3, B), as well as the time range of CAP cycles and sequences. For that purpose, to get the advantage of this work, automatic CAP Phases A and B classification (Mariani et al. 2010, 2013; Ferri et al. 2012; Dhok et al. 2020; Tramonti Fantozzi et al. 2021; Kahana et al. 2023; Sharma et al. 2023; Telangore et al. 2025), its automatic detection of start-end time sample point, and the automatic sleep stage classification in healthy individuals (Dimitriadis et al. 2018b; Jain and G 2024; Chen et al. 2025) and in sleep disorders (Sharma et al. 2021, 2022) are of major importance. The manual annotation by experts of sleep stages and CAP phases is a time-consuming activity and for that reason the clinical

applications of CAP analysis remain limited. Thirdly, due to limitations of the CAP sleep study, we couldn't correlate the extracted features with clinical variables across the sleep disorders.

Conclusions

In the present study, we employed for the very first time, based on authors' knowledge, the healthy control group of this unique database as a common reference for the seven sleep disorders. In this way, we anticipated that the use of robust sleep-disorder, prior effect size weights compared to a common healthy control group, will help parse individual subject and sleep disorder-specific heterogeneity by accounting for individualized profiles of macrostructural-microstructural alterations, and provide sleep disorder-specific sensitivity. The absolute performance of the trained RF model with the proposed SLEIS scores compared to original feature weights validated our hypothesis. The increment of sample size with the use of a large normative lifespan database as a reference is in the right research direction. The investigation of the relationship between EEG features like power spectrum and connectivity and the extracted features presented here like the proposed SLEIS markers, will reveal the neurophysiology of sleep disorders. Also, the correlation of the macrostructural, microstructural features and SLEIS markers should be systematically compared to clinical diagnostic features of sleep disorders. Leveraging diverse methods for automatic sleep stage classification, and automatic detection of start-end time of CAP phases A and B will support the computation of SLEIS markers.

Author contributions

Stavros I Dimitriadis: conceptualization, supervision, data curation, methodology, formal analysis, software, writing (original draft), and performed the machine learning analysis.

Christos Salis: data curation, formal analysis, software, performed the feature extraction analysis, writing (reviewing and editing).

Funding

This research has been conducted in the absence of any funding support.

Conflict of interest

The authors declare that the research was conducted in the absence of any commercial or financial relationships that could be construed as a potential conflict of interest.

Data availability statement

The data supporting the findings of the present study are openly available at the following URL: https:// physionet.org/content/capslpdb/1.0.0/ .

The original features and the SLEIS scores will be released in our github's website upon acceptance of the manuscript.

https://github.com/stdimitr/CAP_Sleep_Disorders/tree/main

Acknowledgments

We would like to acknowledge researchers, staff, and technicians who made this dataset available to the public. Special thanks also to the staff and scientists who keep the Physionet database active.

Figure Captions

Fig.1. An example of a CAP sequence with the enclosed CAP cycles and CAP phases A and B from the first normal subject 1 (n1) extracted from N1 sleep stage. EEG signal was filtered within the 1-12 Hz frequency range using eegfilt function and FIR filtering.

Fig.2. An example of hypnograms and the appearance of CAP sequences for each class denotes as red dots.

A - subject n1, B - subject brux1, C - subject ins1, D - subject narco1

E - subject nfle1, F - subject plm1, G - subject rbd1, H - subject sdb1

Fig.3. Mean and standard deviations of the seven most discriminative features

across the normal group and the seven sleep disorders.

Fig.4. Mean and standard deviations of the four groups of features across the seven sleep disorders.

Fig.5. Mean and standard deviations of the nine most discriminative features across the seven sleep disorders.

Figure 1

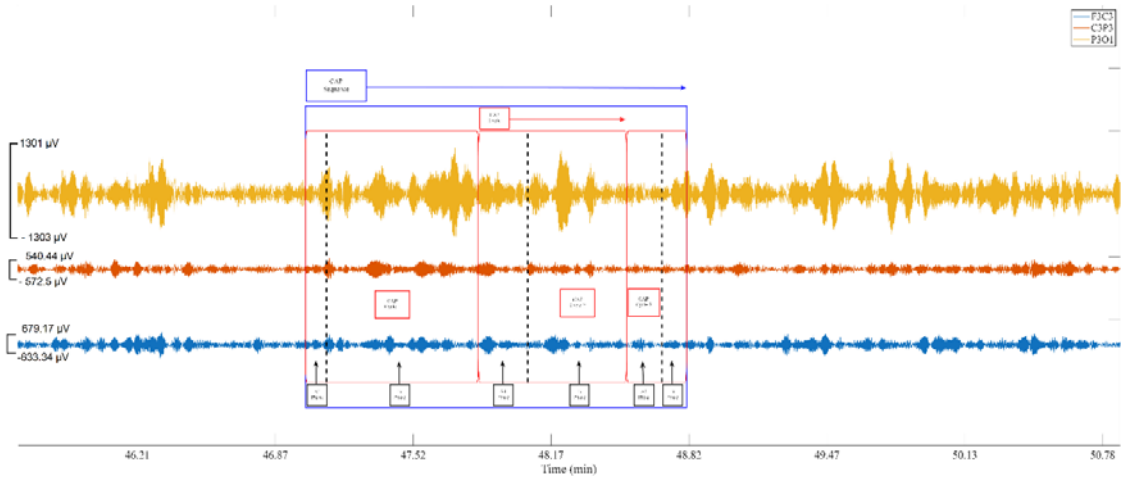

Figure 2

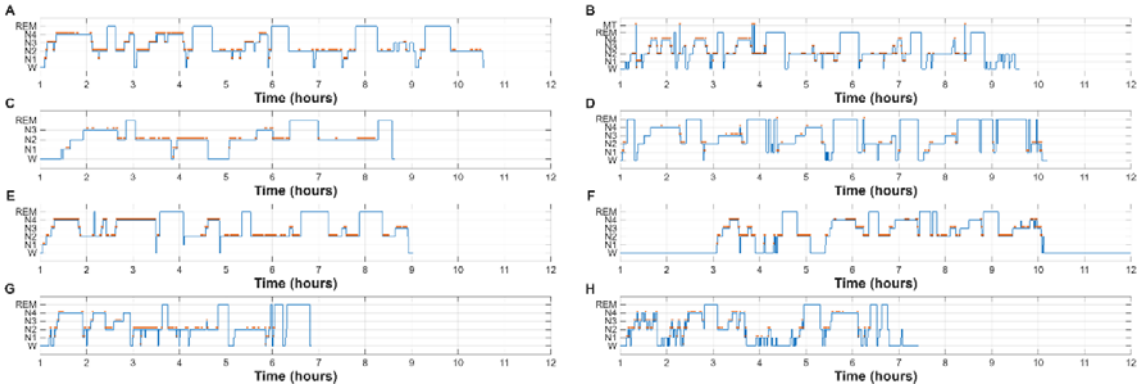

Figure 3

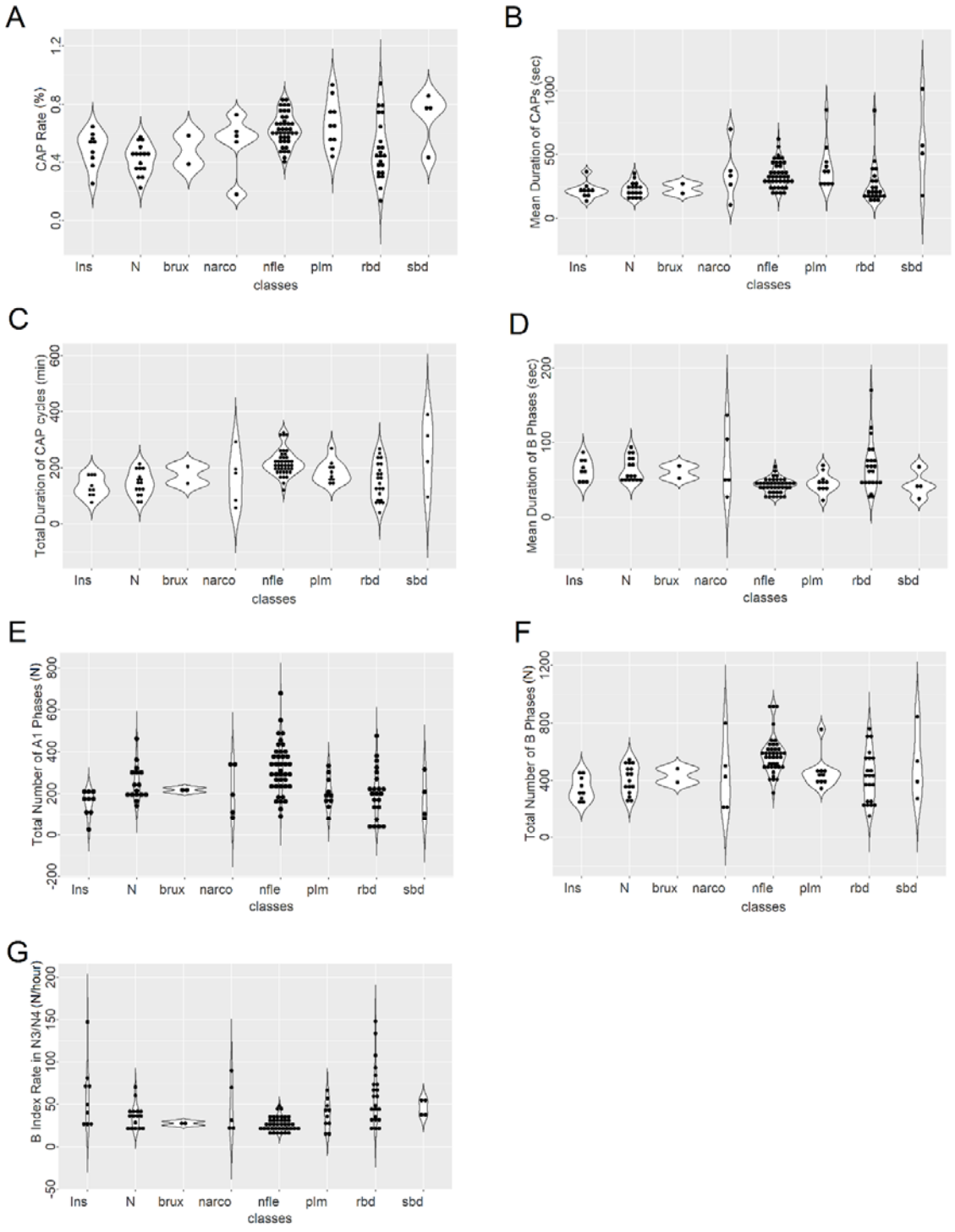
A
CAP Rate (%)
0.0
0.4
0.8
1.2
Ins
N
brux
narco
nfle
plm
rbd
sbd
classes
B
Mean Duration of CAPs (sec)
0
500
1000
Ins
N
brux
narco
nfle
plm
rbd
sbd
classes
C
Total Duration of CAP cycles (min)
0
200
400
600
Ins
N
brux
narco
nfle
plm
rbd
sbd
classes
D
Mean Duration of B Phases (sec)
0
100
200
Ins
N
brux
narco
nfle
plm
rbd
sbd
classes
E
Total Number of A1 Phases (N)
-200
0
200
400
600
800
Ins
N
brux
narco
nfle
plm
rbd
sbd
classes
F
Total Number of B Phases (N)
0
400
800
1200
Ins
N
brux
narco
nfle
plm
rbd
sbd
classes
G
B Index Rate in N3/N4 (N/hour)
-50
0
50
100
150
200
Ins
N
brux
narco
nfle
plm
rbd
sbd
classes

Figure 4

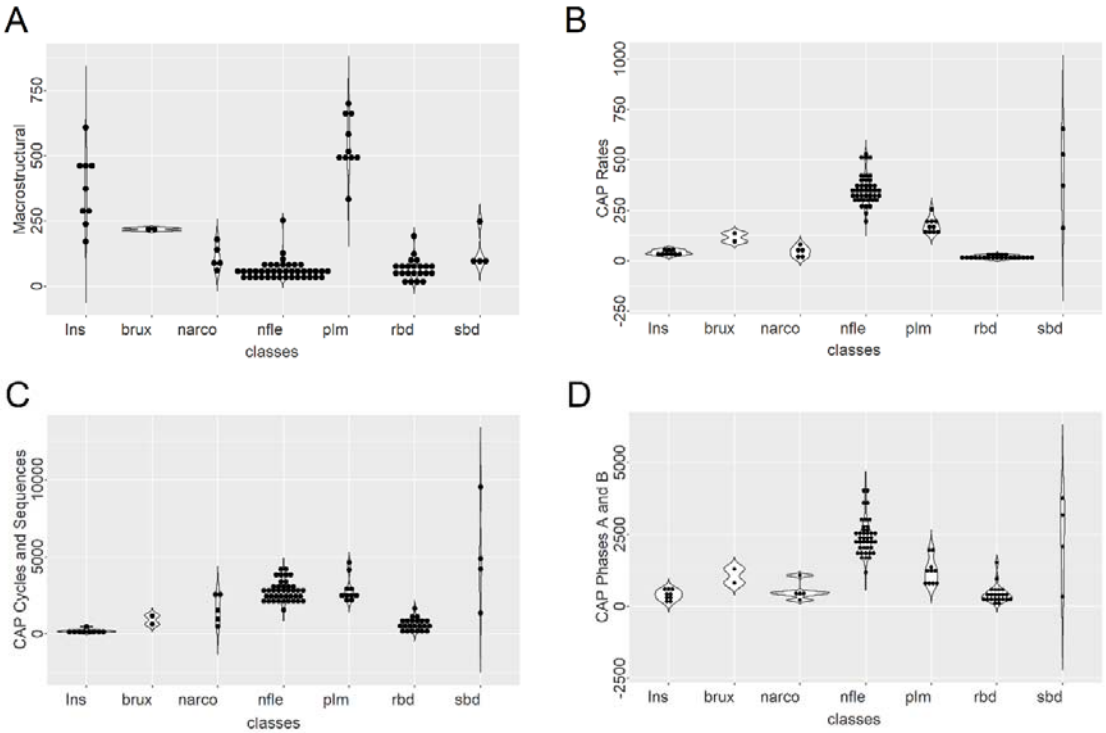
A
Macrostructural
0
250
500
750
Ins
brux
narco
nfle
plm
rbd
sbd
classes
B
CAP Rates
-250
0
250
500
750
1000
Ins
brux
narco
nfle
plm
rbd
sbd
classes
C
CAP Cycles and Sequences
0
5000
10000
Ins
brux
narco
nfle
plm
rbd
sbd
classes
D
CAP Phases A and B
-2500
0
2500
5000
Ins
brux
narco
nfle
plm
rbd
sbd
classes

Figure 5

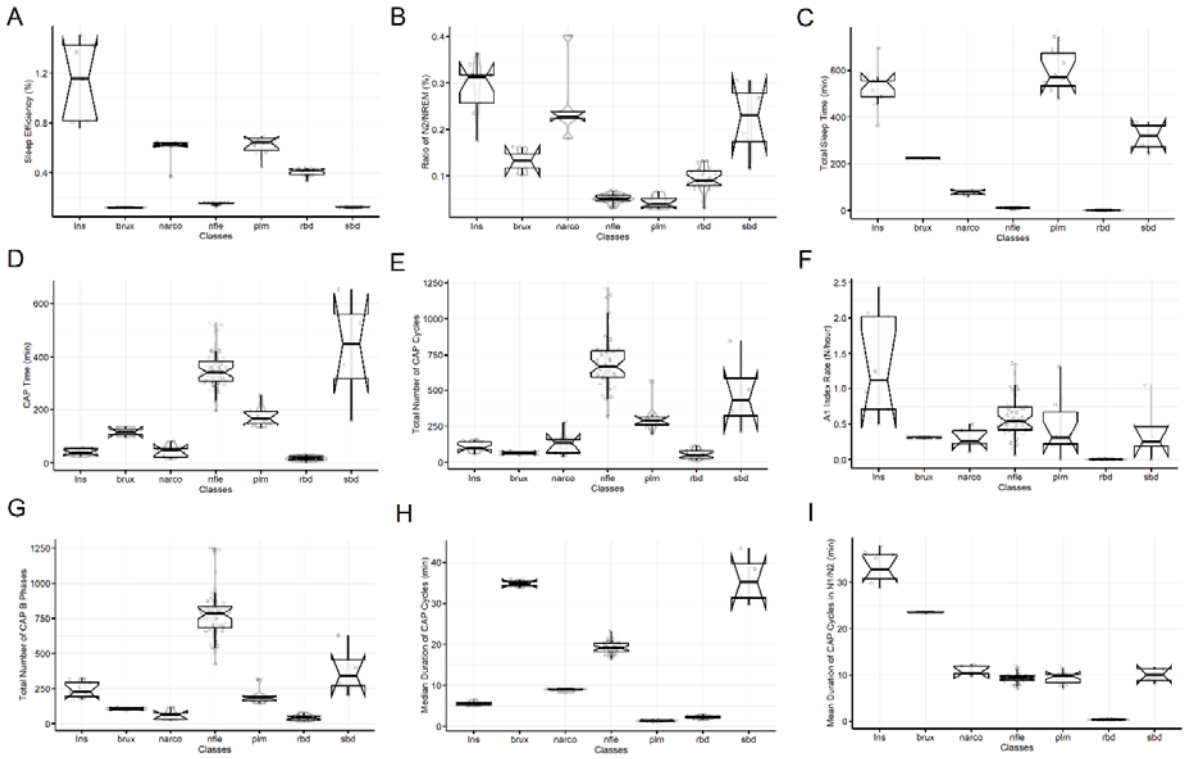

Bibliography

Assadzadeh S, Robinson PA. Necessity of the sleep-wake cycle for synaptic homeostasis: system-level analysis of plasticity in the corticothalamic system. R Soc Open Sci. 2018 Oct 10;5(10):171952.

Bergmann M, Högl B, Stefani A. Clinical neurophysiology of REM parasomnias: Diagnostic aspects and insights into pathophysiology. Clin Neurophysiol Pract. 2024 Jan 10;9:53–62.

Bethlehem RAI, Seidlitz J, White SR, Vogel JW, Anderson KM, Adamson C, et al. Brain charts for the human lifespan. Nature. 2022 Apr 6;604(7906):525–33.

Bidaki R, Zarei M, Khorram Toosi A, Hakim Shooshtari M. A review on genetics of sleep disorders. Iran J Psychiatry Behav Sci. 2012;6(1):12–9.

Breiman L. Random Forests. Springer Science and Business Media LLC. 2001;45:5–32.

Breton-Provencher V, Drummond GT, Sur M. Locus coeruleus norepinephrine in learned behavior: anatomical modularity and spatiotemporal integration in targets. Front Neural Circuits. 2021 Jun 7;15:638007.

Brown RE, Basheer R, McKenna JT, Strecker RE, McCarley RW. Control of sleep and wakefulness. Physiol Rev. 2012 Jul;92(3):1087–187.

Carskadon MA, Dement WC. Normal human sleep: an overview. Principles and practice of sleep medicine. Elsevier; 2005. p. 13–23.

Chen J, Fan X, Ge R, Xiao J, Wang R, Ma W, et al. Towards interpretable sleep stage classification with a multi-stream fusion network. BMC Med Inform Decis Mak. 2025 Apr 14;25(1):164.

Cirelli C, Tononi G. The why and how of sleep-dependent synaptic down-selection. Semin Cell Dev Biol. 2022 May;125:91–100.

Dauvilliers Y, Tafti M. The genetic basis of sleep disorders. Curr Pharm Des. 2008;14(32):3386–95.

Dhok S, Pimpalkhute V, Chandurkar A, Bhurane AA, Sharma M, Acharya UR. Automated phase classification in cyclic alternating patterns in sleep stages using Wigner-Ville Distribution based features. Comput Biol Med. 2020 Apr;119:103691.

Dimitriadis SI, Liparas D, Tsolaki MN, Alzheimer's Disease Neuroimaging Initiative. Random forest feature selection, fusion and ensemble strategy: Combining multiple morphological MRI measures to discriminate among healhy elderly, MCI, cMCI and alzheimer's disease patients: From the alzheimer's disease neuroimaging initiative (ADNI) database. J Neurosci Methods. 2018a May 15;302:14–23.

Dimitriadis SI, Salis C, Linden D. A novel, fast and efficient single-sensor automatic sleep-stage classification based on complementary cross-frequency coupling estimates. Clin Neurophysiol. 2018b Apr;129(4):815–28.

Dimitriadis SI, Salis CI, Liparas D. An automatic sleep disorder detection based on EEG cross-frequency coupling and random forest model. J Neural Eng. 2021 May 24;18(4).

Dimitriadis SI, Simos PG, Fletcher JM, Papanicolaou AC. Typical and aberrant functional brain flexibility: lifespan development and aberrant organization in traumatic brain injury and dyslexia. Brain Sci. 2019 Dec 16;9(12).

Dimitriadis SI. Universal Lifespan Trajectories of Source-Space Information Flow Extracted from Resting-State MEG Data. Brain Sci. 2022 Oct 18;12(10).

Dimitriadis SI. SCZ: A Riemannian schizophrenia diagnosis framework based on the multiplexity of EEG-based dynamic functional connectivity patterns. Comput Biol Med. 2024 Sep;180:108862.

Ferri R, Huber R, Aricò D, Drago V, Rundo F, Ghilardi MF, et al. The slow-wave components of the cyclic alternating pattern (CAP) have a role in sleep-related learning processes. Neurosci Lett. 2008 Feb 27;432(3):228–31.

Ferri R, Rundo F, Novelli L, Terzano MG, Parrino L, Bruni O. A new quantitative automatic method for the measurement of non-rapid eye movement sleep electroencephalographic amplitude variability. J Sleep Res. 2012 Apr;21(2):212–20.

Ghermezian A, Nami M, Shalbaf R, Khosrowabadi R, Nasehi M, Kamali A-M. Sleep Micro-Macro-structures in Psychophysiological Insomnia. PSG Study. Sleep Vigilance. 2023 Apr 16;1–9.

Goldberger AL, Amaral LA, Glass L, Hausdorff JM, Ivanov PC, Mark RG, et al. PhysioBank, PhysioToolkit, and PhysioNet: components of a new research resource for complex physiologic signals. Circulation. 2000 Jun 13;101(23):E215-20.

Halász P, Bódizs R, Parrino L, Terzano M. Two features of sleep slow waves: homeostatic and reactive aspects--from long term to instant sleep homeostasis. Sleep Med. 2014 Oct;15(10):1184–95.

Halász P. The K-complex as a special reactive sleep slow wave - A theoretical update. Sleep Med Rev. 2016 Oct;29:34–40.

Hastings MH, Maywood ES, Brancaccio M. Generation of circadian rhythms in the suprachiasmatic nucleus. Nat Rev Neurosci. 2018 Aug;19(8):453–69.

Hening W. The clinical neurophysiology of the restless legs syndrome and periodic limb movements. Part I: diagnosis, assessment, and characterization. Clin

Neurophysiol. 2004 Sep;115(9):1965–74.

Iber C. The AASM manual for thescoring of sleep and associated events: rules, terminology, and technicalspecifications. 1st ed. USA: Westchester, IL: American Academy of Sleep Medicine; 2007.

Jain R, G RA. Modality-Specific Feature Selection, Data Augmentation and Temporal Context for Improved Performance in Sleep Staging. IEEE J Biomed Health Inform. 2024 Feb 5;28(2):1031–42.

Jones SE, Tyrrell J, Wood AR, Beaumont RN, Ruth KS, Tuke MA, et al. Genome-Wide Association Analyses in 128,266 Individuals Identifies New Morningness and Sleep Duration Loci. PLoS Genet. 2016 Aug 5;12(8):e1006125.

Kahana Y, Aberdam A, Amar A, Cohen I. Deep-Learning-Based Classification of Cyclic-Alternating-Pattern Sleep Phases. Entropy (Basel). 2023 Sep 28;25(10).

Kato T, Montplaisir JY, Guitard F, Sessle BJ, Lund JP, Lavigne GJ. Evidence that experimentally induced sleep bruxism is a consequence of transient arousal. J Dent Res. 2003 Apr;82(4):284–8.

Kjaerby C, Andersen M, Hauglund NL, Ding F, Wang W, Xu Q, et al. Dynamic fluctuations of the locus coeruleus-norepinephrine system underlie sleep state transitions. BioRxiv. 2020 Sep 2;

Lancaster TM, Dimitriadis SI, Perry G, Zammit S, O'Donovan MC, Linden DE. Morphometric Analysis of Structural MRI Using Schizophrenia Meta-analytic Priors Distinguish Patients from Controls in Two Independent Samples and in a Sample of Individuals With High Polygenic Risk. Schizophr Bull. 2022 Mar 1;48(2):524–32.

Liparas D, HaCohen-Kerner Y, Moumtzidou A, Vrochidis S, Kompatsiaris I. News articles classification using random forests and weighted multimodal features. In: Lamas D, Buitelaar P, editors. Multidisciplinary Information Retrieval. Cham: Springer International Publishing; 2014. p. 63–75.

Lo C-C, Chou T, Penzel T, Scammell TE, Strecker RE, Stanley HE, et al. Common scale-invariant patterns of sleep-wake transitions across mammalian species. Proc Natl Acad Sci USA. 2004 Dec 14;101(50):17545–8.

Lombardi F, Gómez-Extremera M, Bernaola-Galván P, Vetrivelan R, Saper CB, Scammell TE, et al. Critical Dynamics and Coupling in Bursts of Cortical Rhythms Indicate Non-Homeostatic Mechanism for Sleep-Stage Transitions and Dual Role of VLPO Neurons in Both Sleep and Wake. J Neurosci. 2020 Jan 2;40(1):171–90.

Mariani S, Bianchi AM, Manfredini E, Rosso V, Mendez MO, Parrino L, et al. Automatic detection of a phases of the cyclic alternating pattern during sleep.

Annu Int Conf IEEE Eng Med Biol Soc. 2010;2010:5085–8.

Mariani S, Grassi A, Mendez MO, Milioli G, Parrino L, Terzano MG, et al. EEG segmentation for improving automatic CAP detection. Clin Neurophysiol. 2013 Sep;124(9):1815–23.

Marquand A, Rutherford S, Wolfers T. Normative modeling for clinical neuroscience. Computational and network modeling of neuroimaging data. Elsevier; 2024. p. 309–29.

Ma MA, Morrison EH. Neuroanatomy, Nucleus Suprachiasmatic. StatPearls. Treasure Island (FL): StatPearls Publishing; 2025.

Martin JM, Andriano DW, Mota NB, Mota-Rolim SA, Araújo JF, Solms M, et al. Structural differences between REM and non-REM dream reports assessed by graph analysis. PLoS ONE. 2020 Jul 23;15(7):e0228903.

Mendez MO, Chouvarda I, Alba A, Bianchi AM, Grassi A, Arce-Santana E, et al. Analysis of A-phase transitions during the cyclic alternating pattern under normal sleep. Med Biol Eng Comput. 2016 Jan;54(1):133–48.

Mieda M. The central circadian clock of the suprachiasmatic nucleus as an ensemble of multiple oscillatory neurons. Neurosci Res. 2020 Jul;156:24–31.

Mogavero MP, DelRosso LM, Lanza G, Bruni O, Ferini Strambi L, Ferri R. The dynamics of cyclic-periodic phenomena during non-rapid and rapid eye movement sleep. J Sleep Res. 2025 Apr;34(2):e14265.

Moore RY. Suprachiasmatic nucleus in sleep-wake regulation. Sleep Med. 2007 Dec;8 Suppl 3:27–33.

Onton JA, Kang DY, Coleman TP. Visualization of Whole-Night Sleep EEG From 2-Channel Mobile Recording Device Reveals Distinct Deep Sleep Stages with Differential Electrodermal Activity. Front Hum Neurosci. 2016 Nov 29;10:605.

Parrino L, Boselli M, Buccino GP, Spaggiari MC, Di Giovanni G, Terzano MG. The cyclic alternating pattern plays a gate-control on periodic limb movements during non-rapid eye movement sleep. J Clin Neurophysiol. 1996 Jul;13(4):314–23.

Parrino L, Boselli M, Spaggiari MC, Smerieri A, Terzano MG. Cyclic alternating pattern (CAP) in normal sleep: polysomnographic parameters in different age groups. Electroencephalogr Clin Neurophysiol. 1998 Dec;107(6):439–50.

Parrino L, Ferri R, Bruni O, Terzano MG. Cyclic alternating pattern (CAP): the marker of sleep instability. Sleep Med Rev. 2012 Feb;16(1):27–45.

Parrino L, Halasz P, Tassinari CA, Terzano MG. CAP, epilepsy and motor events during sleep: the unifying role of arousal. Sleep Med Rev. 2006 Aug;10(4):267–85.

Parrino L, Rausa F, Azzi N, Pollara I, Mutti C. Cyclic alternating patterns and arousals: what is relevant in obstructive sleep apnea? In Memoriam Mario Giovanni Terzano. Curr Opin Pulm Med. 2021 Nov 1;27(6):496–504.

Parrino L, Spaggiari MC, Boselli M, Barusi R, Terzano MG. Effects of prolonged wakefulness on cyclic alternating pattern (CAP) during sleep recovery at different circadian phases. J Sleep Res. 1993 Jun;2(2):91–5.

Poryazova R, Werth E, Parrino L, Terzano MG, Bassetti CL. Cyclic alternating pattern in narcolepsy patients and healthy controls after partial and total sleep deprivation. Clin Neurophysiol. 2011 Sep;122(9):1788–93.

Rutherford S, Fraza C, Dinga R, Kia SM, Wolfers T, Zabihi M, et al. Charting brain growth and aging at high spatial precision. eLife. 2022 Feb 1;11.

Saper CB, Fuller PM, Pedersen NP, Lu J, Scammell TE. Sleep state switching. Neuron. 2010 Dec 22;68(6):1023–42.

Scarpetta S, Morisi N, Mutti C, Azzi N, Trippi I, Ciliento R, et al. Criticality of neuronal avalanches in human sleep and their relationship with sleep macro- and micro-architecture. iScience. 2023 Oct 20;26(10):107840.

Shafiei G, Esper NB, Hoffmann MS, Ai L, Chen AA, Cluce J, et al. Reproducible Brain Charts: An open data resource for mapping brain development and its associations with mental health. Neuron. 2025 Sep 22;

Sharma M, Darji J, Thakrar M, Acharya UR. Automated identification of sleep disorders using wavelet-based features extracted from electrooculogram and electromyogram signals. Comput Biol Med. 2022 Jan 21;143:105224.

Sharma M, Lodhi H, Yadav R, Sampathila N, Swathi KS, Acharya UR. Automated Explainable Detection of Cyclic Alternating Pattern (CAP) Phases and Sub-Phases Using Wavelet-Based Single-Channel EEG Signals. IEEE Access. 2023;11:50946–61.

Sharma M, Tiwari J, Acharya UR. Automatic Sleep-Stage Scoring in Healthy and Sleep Disorder Patients Using Optimal Wavelet Filter Bank Technique with EEG Signals. Int J Environ Res Public Health. 2021 Mar 17;18(6).

Smerieri A, Parrino L, Agosti M, Ferri R, Terzano MG. Cyclic alternating pattern sequences and non-cyclic alternating pattern periods in human sleep. Clin Neurophysiol. 2007 Oct;118(10):2305–13.

Steriade M, Amzica F, Contreras D. Cortical and thalamic cellular correlates of electroencephalographic burst-suppression. Electroencephalogr Clin Neurophysiol. 1994 Jan;90(1):1–16.

Telangore H, Kumar Jha A, Verma P, Sharma M, Sabareesh C, Bhurane AA, et al. Automated identification of cyclic alternating patterns of sleep using fusion of

VGG16 and vision transformer. IEEE Access. 2025;13:106652–72.

Terzano MG, Gatti PL, Manzoni GC, Formentini E, Mancia D. Is the EEG cyclic alternating pattern a true autonomous entity? Analytic study in a case of post-traumatic coma with good prognosis. Eur Neurol. 1982;21(5):324–34.

Terzano MG, Mancia D, Salati MR, Costani G, Decembrino A, Parrino L. The cyclic alternating pattern as a physiologic component of normal NREM sleep. Sleep. 1985;8(2):137–45.

Terzano MG, Parrino L, Boselli M, Spaggiari MC, Di Giovanni G. Polysomnographic analysis of arousal responses in obstructive sleep apnea syndrome by means of the cyclic alternating pattern. J Clin Neurophysiol. 1996 Mar;13(2):145–55.

Terzano MG, Parrino L, Rosa A, Palomba V, Smerieri A. CAP and arousals in the structural development of sleep: an integrative perspective. Sleep Med. 2002 May;3(3):221–9.

Terzano MG, Parrino L, Sherieri A, Chervin R, Chokroverty S, Guilleminault C, et al. Atlas, rules, and recording techniques for the scoring of cyclic alternating pattern (CAP) in human sleep. Sleep Med. 2001 Nov;2(6):537–53.

Terzano MG, Parrino L, Smerieri A, Carli F, Nobili L, Donadio S, et al. CAP and arousals are involved in the homeostatic and ultradian sleep processes. J Sleep Res. 2005 Dec;14(4):359–68.

Terzano MG, Parrino L, Spaggiari MC, Palomba V, Rossi M, Smerieri A. CAP variables and arousals as sleep electroencephalogram markers for primary insomnia. Clin Neurophysiol. 2003 Sep;114(9):1715–23.

Terzano MG, Smerieri A, Del Felice A, Giglia F, Palomba V, Parrino L. Cyclic alternating pattern (CAP) alterations in narcolepsy. Sleep Med. 2006 Dec;7(8):619–26.

Terzano MG. Mutual cooperationbetween cyclic alternating pattern and major dynamic events ofsleep. Insomnia and imidazopyridines. Amsterdam: Excerpta Medica; 1990. p. 262–70.

Terzano MG. Functional relationship between macro and microstructure of sleep. Phasic events and dynamic organisation of sleep. Phasic events and dynamic organization of sleep. New York: Raven Press; 1991. p. 101–19.

Tramonti Fantozzi MP, Faraguna U, Ugon A, Ciuti G, Pinna A. Automatic Cyclic Alternating Pattern (CAP) analysis: Local and multi-trace approaches. PLoS ONE. 2021 Dec 2;16(12):e0260984.

Troester MM. The AASM manual for the scoring of sleep and associated events: rules, terminology and technical specifications. [Internet]. Version 3. RB B, DT P, AR A, MA A, editors. USA: Darien: American Academy of Sleep Medicine;

2023 Dec. Available from: https://aasm.org/clinical-resources/scoring-manual/

Wang JWJL, Lombardi F, Zhang X, Anaclet C, Ivanov PC. Non-equilibrium critical dynamics of bursts in θ and δ rhythms as fundamental characteristic of sleep and wake micro-architecture. PLoS Comput Biol. 2019 Nov 14;15(11):e1007268.

Wolpert EA. A manual of standardized terminology, techniques and scoring system for sleep stages of human subjects. Arch Gen Psychiatry. 1969 Feb 1;20(2):246.

Zucconi M, Ferini-Strambi L. NREM parasomnias: arousal disorders and differentiation from nocturnal frontal lobe epilepsy. Clin Neurophysiol. 2000 Sep;111:S129–35.

Zucconi M, Oldani A, Smirne S, Ferini-Strambi L. The macrostructure and microstructure of sleep in patients with autosomal dominant nocturnal frontal lobe epilepsy. J Clin Neurophysiol. 2000 Jan;17(1):77–86.